

Effects of Mesenchymal Stem Cell-derived Exosomes on Oxidative Stress Responses in Skin Cells

Takaaki Matsuoka

Omotesando Helene Clinic

Keita Takanashi (✉ keita.takanashi@yok.hamayaku.ac.jp)

Yokohama University of Pharmacy <https://orcid.org/0000-0001-8104-5179>

Katsuaki Dan

Division of Research and Development, Research Organization of Biological Activity

Kenichi Yamamoto

Real mate Co. Ltd.

Koji Tomobe

Pathophysiology, Yokohama University of Pharmacy

Tatsuo Shinozuka

Pathophysiology, Yokohama University of Pharmacy

Research Article

Keywords: Exosome, mesenchymal stem cells, oxidative stress, reactive oxygen species, β -galactosidase, fibroblasts

Posted Date: March 10th, 2021

DOI: <https://doi.org/10.21203/rs.3.rs-268923/v1>

License:   This work is licensed under a Creative Commons Attribution 4.0 International License.

[Read Full License](#)

Abstract

Background: The mechanism by which reactive oxygen species (ROS) produced by oxidative stress promote cellular senescence has been studied in detail. This study aimed to verify the preventive or therapeutic effects of mesenchymal stem cell-derived exosomes (MSC-Ex) on the production of ROS induced by oxidative stress in human skin fibroblasts and clarify the mechanisms that promote cellular senescence.

Methods: In a system where H_2O_2 was applied to skin fibroblasts, we assessed the effects of the application of MSC-Ex before and after oxidative stress and measured the fluctuations in several signaling molecules involved in subsequent intracellular stress responses. Exosomes were isolated from MSCs (MSC-Ex) and normal human dermal fibroblasts (NHDFs, NHDF-Ex) before and after exposure to H_2O_2 . NHDFs were treated with exosomes before and after exposure to H_2O_2 .

Results: mRNA expression (aquaporin-1 and aquaporin-3) and hyaluronan secretion associated with skin moisturization were reduced by H_2O_2 treatment, whereas MSC-Ex reversed these effects. The cellular senescence induced by H_2O_2 was also reproduced in fibroblasts. Specifically, the downregulation of SIRT1 led to increased acetylated p53 expression over time, which induced the expression of p21, a downstream molecule of p53, and arrested the cell cycle, leading to cell senescence. MSC-Ex enhanced these signal transduction systems. MSC-Ex was also effective at blocking the increase of β -galactosidase activity and accumulation of ROS in cells. This effect was stronger than that of NHDF-Ex.

Conclusion: MSC-Ex were found to act defensively against epidermal and cellular senescence induced by oxidative stress.

Introduction

The free radical theory states cellular damage induced by oxidative stress throughout the body is one of the main causes of various senile diseases and that this damage changes biological structures and reduces function [1]. In particular, damage to DNA, proteins, and lipids by reactive oxygen species (ROS) generated following exposure to hydrogen peroxide plays an important role in accelerating aging and the development and severity of senile diseases [2, 3]. The mechanism by which ROS generated by oxidative stress accelerates cellular senescence has been examined in detail, and various phenomena in cells and the roles of various molecules are being clarified. DNA fragmentation [4], shortening of telomeric regions [5], and poly Adenosine diphosphate-ribose polymerase activation are induced; NAD⁺ is consumed [6]; and SIRT1 activity is reduced [7]. In addition, experiments using H_2O_2 as an oxidative stress in human embryonic lung fibroblasts strongly suggested that decreased SIRT1 activity leads to increased acetylated p53 expression over time and induces the expression of p21, a downstream molecule of p53, leading to cell senescence because of cell cycle arrest [8].

Aquaporin (AQP)-1 and AQP-3 were recently implicated in the activation of skin fibroblasts, and oxidative stress has also been demonstrated to reduce their expression [9]. H_2O_2 is also transported into cells by AQP-3, regulating cell signaling as a second messenger, and AQP-3 dysregulation is essential for various skin conditions [10].

As regenerative medicine advances, it has been reported that autologous mesenchymal stem cells (MSCs) can be cultured *in vitro* and injected into the body to promote the regeneration of damaged tissues [11]. There is also accumulating evidence that exosomes, in addition to stem cells, have therapeutic effects in a variety of disease models [12]. Specifically, exosomes derived from progenitor adipocytes stimulated cell proliferation *in vitro* in wound-healing models [13]. In addition, exosomes have exhibited beneficial effects in models of kidney [14–18], heart [19–21], brain [22–24], and lung diseases [25–27] such as growth promotion of target cells or suppression of apoptosis, but the mechanism has not been elucidated. Although autologous stem cells are used in the cosmetic surgery field as an anti-aging modality, there is little evidence supporting their moisturizing and anti-aging effects on skin cells.

This study aimed to verify the preventive or therapeutic effects of mesenchymal stem cell-derived exosomes (MSC-Ex) on the production of ROS induced by oxidative stress in human skin fibroblasts and clarify the mechanisms that promote cellular senescence. In a system in which H_2O_2 was applied to skin fibroblasts, we assessed the effects of the application of MSC-Ex before and after oxidative stress and measured the fluctuations in several signaling molecules involved in subsequent intracellular stress responses. In this study, we found that MSC-Ex protect against oxidative stress-induced ROS production and cellular senescence.

Materials And Methods

Cell cultures

Human MSCs from adipose tissue (C-12977) and dedicated medium (C-28009), normal human dermal fibroblasts (NHDFs) from juvenile foreskin (C-12300) and dedicated medium (C-23020), and normal human epidermal keratinocytes from juvenile foreskin (single donor, C-12001) and dedicated medium (C-20111) were all purchased from Promo Cell. All media were supplemented with 10% fetal bovine serum (Carson, CA, USA), penicillin (100 U ml^{-1}), streptomycin ($100\text{ }\mu\text{g ml}^{-1}$), and kanamycin ($10\text{ }\mu\text{g ml}^{-1}$). Cells were cultured in an incubator at 37°C under 5% CO_2 and used in the experiments.

Biochemical reagents

H_2O_2 and other reagents were purchased from Wako Pure Chemical Industry Co., Ltd.

Extracting, quantifying, and adding exosomes

MSCs and fibroblasts were cultured for 7 days in culture flasks, and culture supernatant was collected from the cells when they reached approximately 80% confluency, with cellular debris removed via centrifugation (12,000 rpm, 15 min). The supernatant was stored at 4°C until exosome isolation. A MiRCURY Exosome Isolation Kit (Product #: 300102; manufactured by EXIQON) was used to isolate exosomes present in the culture medium. Isolated exosome levels were measured using CD9/CD63 enzyme-linked immunosorbent assay (ELISA) kits (for human exosome assays). Isolated exosomes were added to the culture medium at a 1/100 volume (final level, 100 pg ml⁻¹) and incubated for 4 h. These EX-containing media were named MSC-derived exosomes (MSC-Ex) and NHDF-derived exosomes (NHDF-Ex).

Oxidative stress treatment and exosome exposure in cells

NHDFs were incubated for 2 h in medium supplemented with 0.2 mM H₂O₂, washed with PBS, and then incubated in conventional medium [28]. Conversely, the preventive effects of exosomes were investigated by incubating NHDFs with MSC-Ex for 6 h, washing the cells with PBS, and then treating them with 0.2 mM H₂O₂ for 2 h in the same manner. Cells or culture medium was collected at various times after incubation. Total RNA was extracted from cells after exosome and H₂O₂ treatment, and culture supernatants were used for hyaluronan measurements. In addition, measurements of p21 mRNA expression were also performed after 16 h of exosome exposure and 2 h of H₂O₂ stress.

Wound-healing effects

Wound-healing effects were examined using a CytoSelect 24-well Wound-Healing Assay Kit (Cell Biolabs, Inc. San Diego, CA, USA). In the assay, a wound field was created near the center of NHDF cultures for 48 h using an insert placed in the 24-well plate. Thereafter, the cells were cultured for 48 h in culture medium containing various exosomes and then stained with DAPI to observe their growth via fluorescence microscopy, and images were acquired. The effect was measured as the percent closure (migrated cell surface area/total surface area × 100).

Cell growth-promoting effect

NHDFs were cultured in the presence of exosomes and oxidative stress molecules, and the cells and culture medium were recovered at various times. The total number of cells and the number of surviving cells were counted using Countess cell counting chamber slides (Thermo Fisher Scientific K. K. Tokyo, JAPAN) and a CytoTox-ONE Assay Kit (Promega, Madison, WI, USA), respectively (n = 3/group).

Quantitation of mRNA by quantitative RT-PCR (qRT-PCR)

The mRNA levels of AQP-1, AQP-3[29], SIRT-1 [30], p53 [31], and p21 [32] in NHDFs were measured using the one-step qRT-PCR method. The mRNA level of glyceraldehyde-3-phosphate dehydrogenase (GAPDH) was also measured as an internal control [33].

qRT-PCR was performed in the final volume of 20 μ l of solution containing 10 μ l of 2 \times Luna Universal One-Step Reaction Mix, 1 μ l of Luna WarmStart[®] RT Enzyme Mix, 2 μ l of total RNA solution, 1.6 μ l of the primer pair mix (0.4 μ M of each primer), and 7.3 μ l of H₂O under the following conditions: 55°C for 10 min for reverse transcription and 95°C for 1 min for initial denaturation, followed by 45 cycles of 95°C for 10 s and 60°C for 30 s. The relative gene expression was calculated using the $\Delta\Delta$ Ct method [34], and GAPDH gene expression was used for normalization. The primers used in qRT-PCR are shown in Table I. Significant differences were judged when $\Delta\Delta$ Ct > 2.

Hyaluronan production (ELISA) related to skin-moisturizing effects

Hyaluronan levels were assessed using an ELISA kit (R&D Systems, Inc., Minneapolis, MN, USA) according to the manufacturer's instructions.

Effects of oxidative stress on the induction of cellular senescence

Various exosomes were continuously added to NHDFs under oxidative stress, and cellular senescence was examined microscopically using a SPiDER- β Gal kit (SG03; Dojindo, Kumamoto, Japan).

The abundance of senescent cells was evaluated by quantifying the amount of fluorescence in the acquired images. Fluorescent ROS levels were quantified using ImageJ software. Data were shown as the fluorescence intensity (excitation, 488 nm; emission, 590 nm).

Measurement of intracellular ROS production

Intracellular ROS levels were measured using the fluorescent probe CM-H₂DCFDA (Molecular Probes Inc., Eugene, OR, USA). NHDFs were washed with PBS and then incubated with 1 μ M fluorescent probe at 37°C for 60 min. Intracellular ROS levels were assessed according to the fluorescence intensity using a microplate reader (SYNERGY/HT, BioTek, Japan).

Statistical analysis

All results are presented as the mean \pm SD. Statistical significance was determined using one-way analysis of variance, and differences were considered statistically significant when $P < 0.05$.

Results

Cell proliferation-promoting and wound-healing effects of exosomes

The effects of exosomes on the growth of cultured NHDFs were studied. MSC-Ex tended to more strongly induce cell proliferation than NHDF-Ex during the observations (Fig. 1 a).

We investigated whether MSC-Ex has wound-healing effects. As shown in Fig. 1b (mean of five samples per group), wound closure tended to be improved by exposure to NHDF-Ex ($18 \pm 7\%$) and MSC-Ex ($21 \pm 8\%$) compared with the findings in untreated NHDFs ($15 \pm 4\%$), but the differences were not significant.

Effects Of Oxidative Stress On Cell Survival

Treatment of NHDFs with exosomes had no particular effect on survival, but the survival of cells treated with $0.2 \text{ mM H}_2\text{O}_2$ was reduced by 88%. Exposure to exosomes following oxidative stress had no effect on viability, whereas cells treated with MSC-Ex prior to exposure to oxidative stress exhibited significantly improved survival ($P < 0.001$). In addition, MSC-Ex had a significantly stronger effect on cell survival following exposure to oxidative stress than NHDF-Ex ($P < 0.01$) (Fig. 2).

Secretion-stimulating effects of AQPs and involvement of hyaluronan in NHDF activation

Regarding factors involved in skin moisturization, the mRNA expression of AQP-1 and AQP-3 as determined using qRT-PCR are shown in Fig. 3.

The results illustrated that AQP-1 and AQP-3 mRNA levels were decreased by oxidative stress in NHDFs. Meanwhile, exosomes prevented these effects of oxidative stress when used before or after exposure to H_2O_2 , and MSC-Ex exerted stronger effects than NHDF-Ex (Fig. 3).

The amounts of hyaluronan secreted in the culture supernatant by fibroblasts as determined using ELISA are shown in Fig. 4. The amount of hyaluronan secreted by fibroblasts was also decreased by oxidative stress, but its secretion tended to be more strongly restored by MSC-Ex treatment than by NHDF-Ex treatment (Fig. 4).

Effect On Cellular Senescence Due To Oxidative Stress

The mRNA levels of molecules involved in intracellular signaling were quantified.

Oxidative stress reduced SIRT1 expression ($\Delta\Delta\text{Ct} = -4.8$), whereas MSC-Ex treatment restored its expression ($\Delta\Delta\text{Ct} = 2.5$; $P < 0.001$ vs. H_2O_2). The effects of MSC-Ex were stronger when administered prior to oxidative stress ($\Delta\Delta\text{Ct} = -0.3$). The decreased activity of SIRT1 resulted in increased p53 expression

($\Delta\Delta\text{Ct} = 19.9$), whereas the expression of p21, a downstream molecule of p53, was not changed at 6 h ($\Delta\Delta\text{Ct} = 1.3$, data not shown), although induction was observed at 16 h ($\Delta\Delta\text{Ct} = 17.0$). The effect of exosomes was not strongly inhibited after oxidative stress, but the effect was strongly resistant to oxidative stress when MSC-Ex were administered prior to exposure to the stress (p53, $\Delta\Delta\text{Ct} = 14.1$, $P < 0.05$; p21, $\Delta\Delta\text{Ct} = 8.5$, $P < 0.001$; Fig. 5). β -Galactosidase activity was also measured using the SPiDER- β Gal probe as an indicator of cellular senescence (Fig. 6). Oxidative stress increased the fluorescence intensity of the probe to 4730 arbitrary units (AU), compared with 613 AU in unstressed cells. Treatment with NHDF-Ex before and after exposure oxidative stress did not significantly reduce the fluorescence of the probe (pretreatment, 4381 AU; after treatment, 4567 AU), whereas MSC-Ex exerted a significant inhibitory effect both before and after exposure to oxidative stress (pretreatment, 3403 AU; after treatment, 3730 AU).

Inhibitory Effect Of Exosomes On Intracellular Ros Production

We investigated the inhibitory effects of exosomes on ROS production induced by H_2O_2 exposure (Fig. 7). The intracellular intensity of the fluorescent probe increased to 16,300 AU following exposure to H_2O_2 , compared with 2310 AU in unstressed cells. Treatment with NHDF-Ex had no significant effect on ROS production irrespective of their use before or after oxidative stress exposure, whereas MSC-Ex significantly inhibited ROS production when used both before and after treatment with H_2O_2 (pretreatment, 11,230 AU; after treatment, 12,600 AU).

Discussion

In this study, we examined at first the effects of exosomes secreted by MSCs on the growth and viability of NHDFs.

MSC-Ex did not exert any distinct effects on NHDFs alone such as growth promotion or wound-healing (Fig. 1). In an experimental system in which oxidative stress reduced cell viability by 10% or more, the effect was significantly improved when cells were exposed to MSC-Ex prior to exposure to oxidative stress, and the effect was significantly stronger than that of NHDF-Ex (Fig. 2).

It is known that the fibroblasts moisturize the epidermis, and the existence of AQPs, which are associated with water molecule influx into cells, is noticed. In particular, AQP-1 and AQP-3 are expressed in fibroblasts. It was previously reported that hyaluronan secreted by cells is effective for moisturizing the skin [35]. Indeed, oxidative stress reduced the mRNA expression of AQP-1 and AQP-3 and hyaluronan secretion by the cells, and these effects were reversed by exposure to MSC-Ex. The effects of MSC-Ex were stronger than those of NHDF-Ex, particularly in the presence of hyaluronan.

Initially, when examined 6 h after stress exposure, SIRT1 and p53 expression fluctuated as expected, whereas p21 levels were unchanged. Meanwhile, the 16-h study revealed that p21 expression was elevated, and these effects were suppressed by MSC-Ex. Furukawa et al. clarified the mechanisms by which acetylated p53 expression is increased over time following the downregulation of SIRT1, thereby inducing the expression of p21 and leading to cellular senescence via cell cycle arrest [8]. p53 acetylation was not examined in this study, but the findings appeared to support the free radical theory in part.

β -Galactosidase activity and intracellular ROS production were measured as indicators of cellular senescence. MSC-Ex reversed the effects of oxidative stress on both of these variables.

The results demonstrated that exosomes reversed the changes in signal transduction that were induced by H₂O₂ and prevented oxidative stress-induced cellular senescence. Moreover, the observations indicate that the exosomes released by NHDFs themselves have some effect; whereas, those secreted by stem cells may be a part of the defense mechanisms that mediate effects on fibroblasts at distant sites.

Although the mechanism responsible for difference in effects between NHDF-Ex and MSC-Ex is unclear, it was clarified that exosomes act defensively against epidermal and cellular senescence. In the future, novel anti-aging therapies for the skin could be developed from the molecular findings in this study.

Declarations

Acknowledgment

This study was supported by grants from Omotesando Helene Clinic and STEMCELL Ltd.

Conflict of Interest

The authors have no financial interest or conflicts of interest.

Availability of data and material

Not applicable.

Code availability

Not applicable.

Authors' contributions

All authors contributed to this work. T. Matsuoka, K. Dan, K. Yamamoto, K. Tomobe, and T. Shinozuka designed the research. T. Matsuoka, K. Dan, and K. Takanashi performed the experiments and analyzed the results. All authors interpreted the results and designed the research strategy. T. Matsuoka, K. Dan, and K. Takanashi prepared the manuscript.

Ethics approval

Not applicable.

Consent to participate

Not applicable.

Consent for publication

Not applicable.

References

1. Harman D (2006) Free radical theory of aging: an update: increasing the functional life span. *Ann N Y Acad Sci* 1067:10–21
2. Kawanishi S, Hiraku Y, Oikawa S (2001) Mechanism of guanine-specific DNA damage by oxidative stress and its role in carcinogenesis and aging. *Mutat Res* 488:65–76
3. Saxena S, Vekaria H, Sullivan PG, Seifert AW (2019) Connective tissue fibroblasts from highly regenerative mammals are refractory to ROS-induced cellular senescence. *Nat Commun* 10:4400
4. Ben-Porath I, Weinberg RA (2005) The signals and pathways activating cellular senescence. *Int J Biochem Cell Biol* 37:961–976
5. Richter T, von Zglinicki T (2007) A continuous correlation between oxidative stress and telomere shortening in fibroblasts. *Exp Gerontol* 42:1039–1042
6. Mizutani H, Tada-Oikawa S, Hiraku Y, Oikawa S, Kijima M, Kawanishi S (2002) Mechanism of apoptosis induced by a new topoisomerase inhibitor through the generation of hydrogen peroxide. *J Biol Chem* 277:30684–30689
7. Burnet A, Sweeney LB, Sturgill JF, Chua KF, Greer PL, Lin Y et al (2004) Stress-dependent regulation of FOXO transcription factors by the SIRT1 deacetylase. *Science* 303:2011–2015
8. Furukawa A, Tada-Oikawa S, Kawanishi S, Oikawa S (2007) H₂O₂ accelerates cellular senescence by accumulation of acetylated p53 via decrease in the function of SIRT1 by NAD⁺ depletion. *Cell*

9. Xu Y, Yao H, Wang Q, Xu W, Liu K, Zhang J et al (2018) Aquaporin-3 attenuates oxidative stress-induced nucleus pulposus cell apoptosis through regulating the P38 MAPK pathway. *Cell Physiol Biochem* 2018;50:1687–1697
10. Glady A, Tanaka M, Moniaga CS, Yasui M, Hara-Chikuma M (2018) Involvement of NADPH oxidase 1 in UVB-induced cell signaling and cytotoxicity in human keratinocytes. *Biochem Biophys Res Commun* 14:7–15
11. Kraitchman DL, Tatsumi M, Gilson WD, Ishimori T, Kedziorek D, Walczak P et al (2005) Dynamic imaging of allogeneic mesenchymal stem cells trafficking to myocardial infarction. *Circulation* 112:1451–1461
12. Yin K, Wang S, Zhao RC (2019) Exosomes from mesenchymal stem/stromal cells: a new therapeutic paradigm. *Biomark Res* 7:8
13. Lai RC, Yeo RW, Tan KH, Lim SK (2013) Mesenchymal stem cell exosome ameliorates reperfusion injury through proteomic complementation. *Regen Med* 8:197–209
14. Bruno S, Grange C, Deregibus MC, Calogero RA, Saviozzi S, Collino F et al (2009) Mesenchymal stem cell-derived microvesicles protect against acute tubular injury. *J Am Soc Nephrol* 20:1053–1067
15. Gatti S, Bruno S, Deregibus MC, Sordi A, Cantaluppi V, Tetta C et al (2011) Microvesicles derived from human adult mesenchymal stem cells protect against ischaemia-reperfusion-induced acute and chronic kidney injury. *Nephrol Dial Transplant* 26:1474–1483
16. Bruno S, Grange C, Collino F, Deregibus MC, Cantaluppi V, Biancone L et al (2012) Microvesicles derived from mesenchymal stem cells enhance survival in a lethal model of acute kidney injury. *PLoS One* 7:e33115
17. He J, Wang Y, Sun S, Yu M, Wang C, Pei X et al (2012) Bone marrow stem cells-derived microvesicles protect against renal injury in the mouse remnant kidney model. *Nephrology* 17:493–500
18. Zhou Y, Xu H, Xu W, Wang B, Wu H, Tao Y et al (2013) Exosomes released by human umbilical cord mesenchymal stem cells protect against cisplatin-induced renal oxidative stress and apoptosis in vivo and in vitro. *Stem Cell Res Ther* 4:34
19. Lai RC, Arslan F, Lee MM, Sze NSK, Choo A, Chen TS et al (2010) Exosome secreted by MSC reduces myocardial ischemia/reperfusion injury. *Stem Cell Res* 4:214–222
20. Lai RC, Arslan F, Tan SS, Tan B, Choo A, Lee MM et al (2010) Derivation and characterization of human fetal MSCc: An alternative cell source for large-scale production of cardioprotective microparticles. *J Mol Cell Cardiol* 48:1215–1224
21. Arslan F, Lai RC, Smeets MB, Akeroyd L, Choo A, Agnor EN et al (2013) Mesenchymal stem cell-derived exosomes increase ATP levels, decrease oxidative stress and activate P13K/Akt pathway to enhance myocardial viability and prevent adverse remodeling after myocardial ischemia/reperfusion injury. *Stem Cell Res* 10:301–312
22. Xin H, Li Y, Buller B, Katakowski M, Zhang Y, Wang X et al (2012) Exosome mediated transfer of miR-133b from multipotent mesenchymal stromal cells to neural cells contributes to neurite outgrowth.

Stem Cells 30:1556–1564

23. Xin H, Li Y, Liu Z, Wang X, Shang X, Cui Y et al (2013) Mir-133b promotes neural plasticity and functional recovery after treatment of stroke with multipotent mesenchymal stromal cells in rats via transfer of exosome-enriched extracellular particles. *Stem Cells* 31:2737–2746
24. Xin H, Li Y, Cui Y, Yang JJ, Zhang ZG, Chopp M (2013) Systemic administration of exosomes released from mesenchymal stromal cells promote functional recovery and neurovascular plasticity after stroke in rats. *J Cereb Blood Flow Metab* 33:1711–1715
25. Lee C, Mitsialis SA, Aslam M, Vitali SH, Vergadi E, Konstantinou G et al (2012) Exosomes mediate the cytoprotective action of mesenchymal stromal cells on hypoxia-induced pulmonary hypertension. *Circulation* 126:2601–2611
26. Zhu Y, Feng X, Abbott J, Fang X, Hao Q, Monsel A et al (2014) Human mesenchymal stem cell microvesicles for treatment of Escherichia coli endotoxin-induced acute lung injury in mice. *Stem Cells* 32:116–125
27. Islam MN, Das SR, Emin MT, Wei M, Sun L, Westphalen K et al (2012) Mitochondrial transfer from bone-marrow-derived stromal cells to pulmonary alveoli protects against acute lung injury. *Nat Med* 18:759–765
28. Kartal B, Akcay A, Palabiyik B (2018) Oxidative stress upregulates the transcription of genes involved in thiamine metabolism. *Turk J Biol* 42:447–452
29. Brundl J, Wallinger S, Breyer J, Weber F, Evert M, Georgopoulos NT et al (2018) Expression, localization and potential significance of aquaporins in benign and malignant human prostate tissue. *BMC Urol* 18:75
30. Hajighasem A, Farzanegi P, Mazaheri Z, Naghizadeh M, Salehi G (2018) Effects of resveratrol, exercises and their combination on Farnesoid X receptor, Liver X receptor and Sirtuin 1 gene expression and apoptosis in the liver of elderly rats with nonalcoholic fatty liver. *Peer J* 6:e5522
31. Okoye JO, Ngokere AA, Onyenekwe CC, Erinle CA (2019) Comparable expression of miR-let-7b, miR-21, miR-182, miR-145, and p53 in serum and cervical cells: Diagnostic implications for early detection of cervical lesions. *Int J Health Sci (Qassim)* 13:29–38
32. Wang T, Liu J, Li S, Yuan Z, Huang X (2019) Effects of knockout of lincRNA-p21 on the proliferation, migration and invasion ability of HepG2 liver cancer cells. *Oncol Lett* 17:5103–5107
33. Chen YH, Chen ZW, Li HM, Yan XF, Feng B (2018) AGE/RAGE-induced EMP release via the NOX-Derived ROS pathway. *J Diabetes Res* 2018:6823058
34. Kenneth JL, Thomas DS (2001) Analysis of relative gene expression data using real-time quantitative PCR and the 2- $\Delta\Delta$ Ct method. *Methods* 25:402–408
35. Sundaram H, Cegielska A, Wojciechowska A, Delobel P (2018) Prospective, randomized, investigator-blinded, split-face evaluation of a topical crosslinked hyaluronic acid serum for post-procedural improvement of skin quality and biomechanical attribute. *J Drugs Dermatol* 17:442–450

Tables

Table 1
Primers for PCR

Gene	Primer	References
AQP-1	Forward TCT GTA GCC CTT GGA CAC CT Reverse CAA AGG ACC GAG CAG GGT TA	29
AQP-3	Forward TGC TAC CTA CCC CTC TGG AC Reverse GCC AGC ACA CAC ACG ATA AG	29
SIRT-1	Forward GAG TTG TGT GTA GGT TAG GTG G Reverse AAA TAT GAA GAG GTG TTG GTG G	30
P53p53	Forward GCT CAA GAC TGG CGC TAA AA Reverse GTG ACT CAG AGA GGA CTC AT	31
P21p21	Forward CCC GGG CTT GTC TTT TGT T Reverse GAG TGG GTG GCT CAC TCT TCT G	32
GAPDH	Forward AGG GCT GCT TTT AAC TCT GGT Reverse CCC CAC TTG ATT TTG GAG GGA	33
AQP, aquaporin; GAPDH, glyceraldehyde-3-phosphate dehydrogenase		

Figures

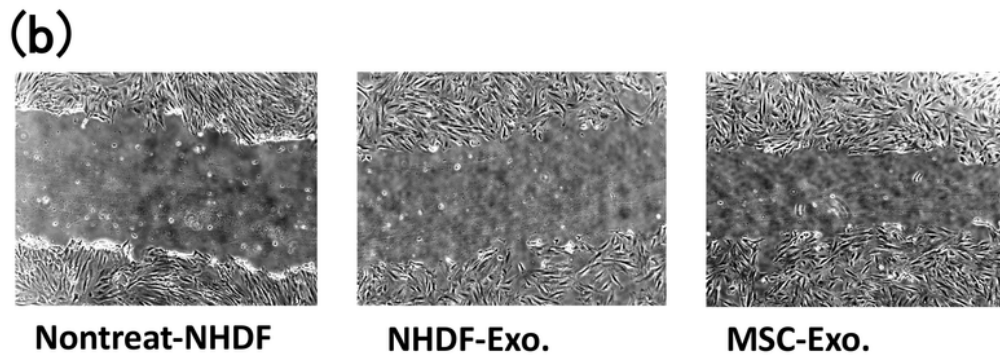
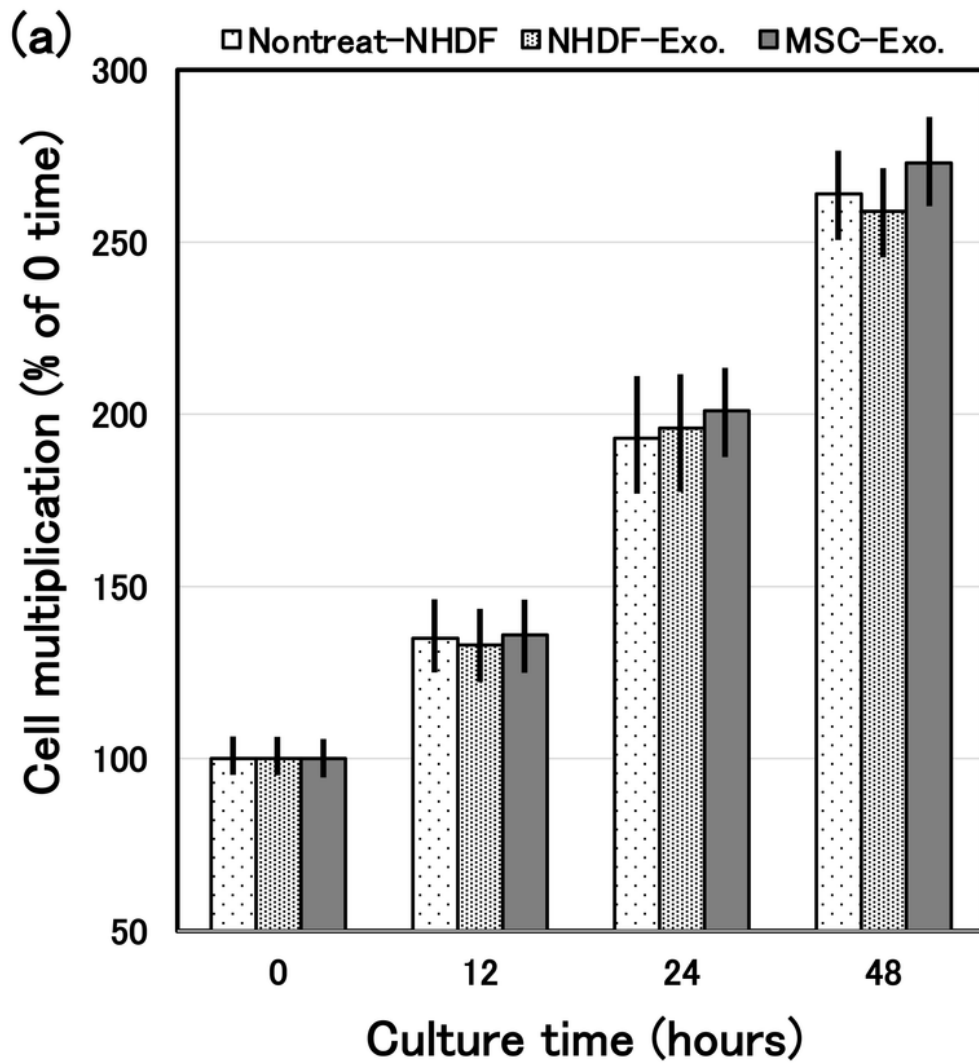


Figure 1

Cell growth and wound-healing in vitro. Normal human dermal fibroblasts (NHDFs) were co-cultured with NHDF exosomes (NHDF-Ex) or mesenchymal stem cell exosomes (MSC-Ex). (a) Cell growth assay. (b) Wound-healing assay.

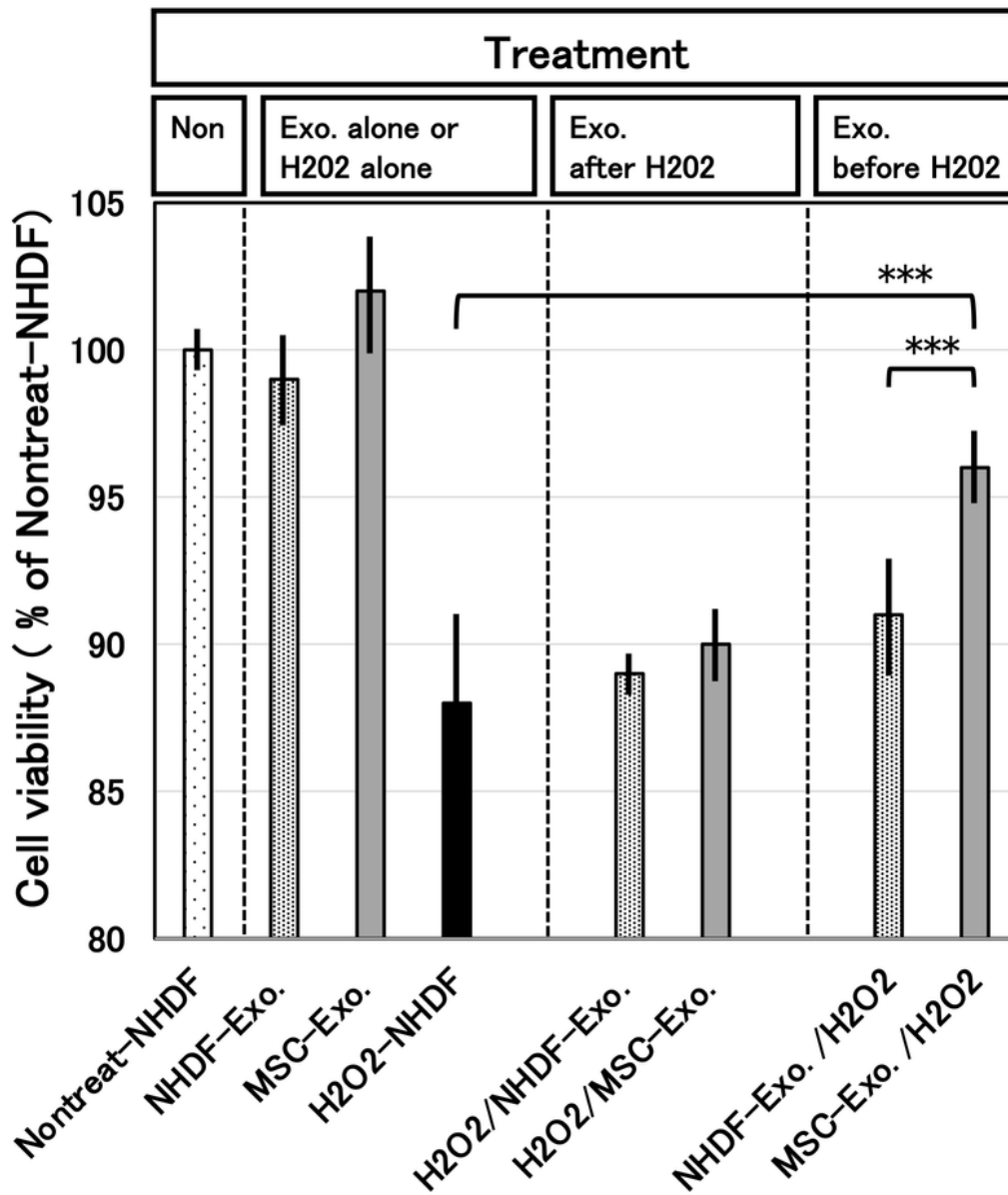


Figure 2

Viability of normal human dermal fibroblasts (NHDFs). NHDFs were treated as described in the Materials and Methods, and cell viability was assessed at 48 h. **P < 0.01, *** P < 0.001.

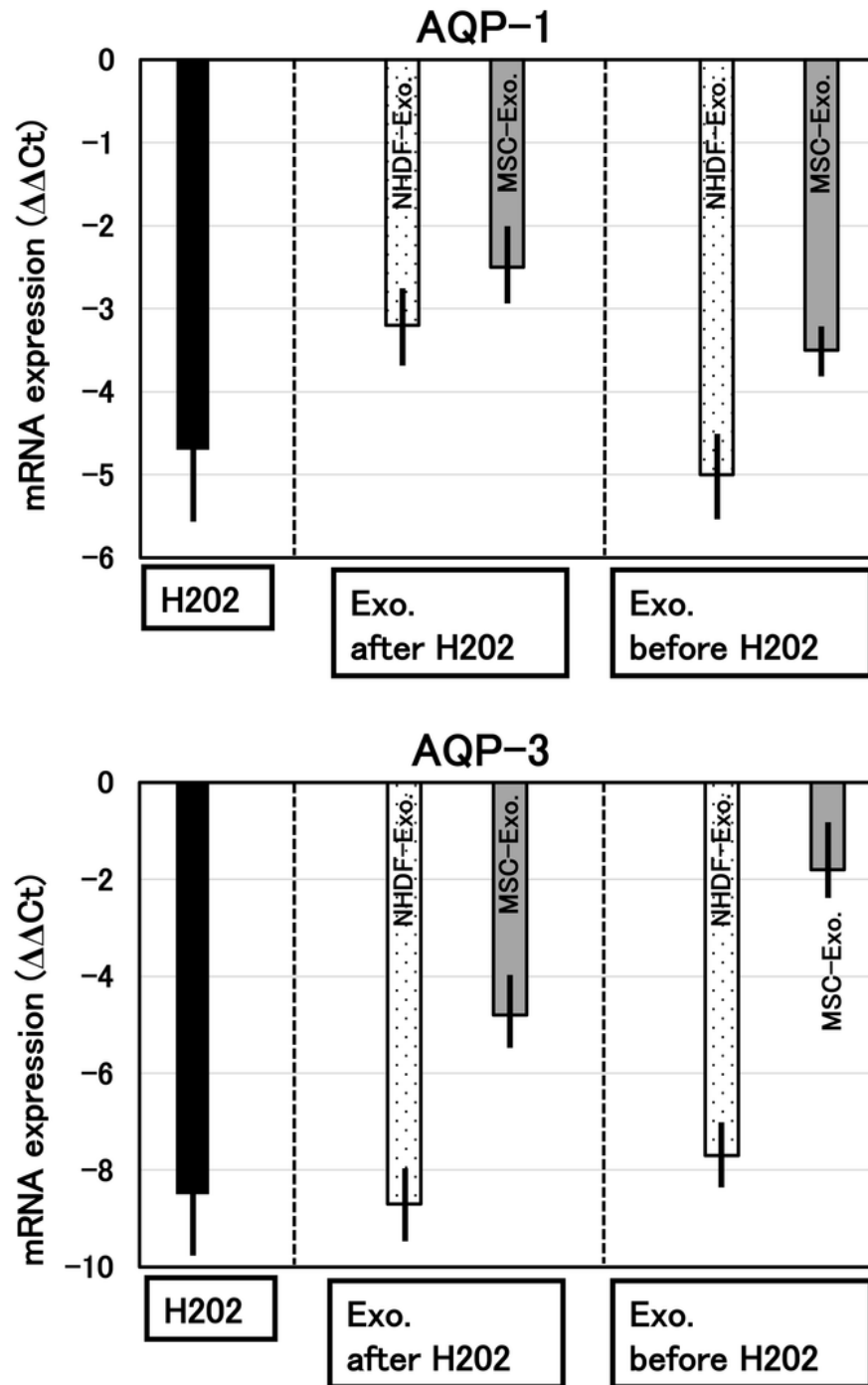


Figure 3

mRNA expression levels of aquaporins (AQPs) in normal human dermal fibroblasts. The mRNA levels of AQP-1 and AQP-3 were determined by qRT-PCR and presented as $\Delta\Delta Ct$.

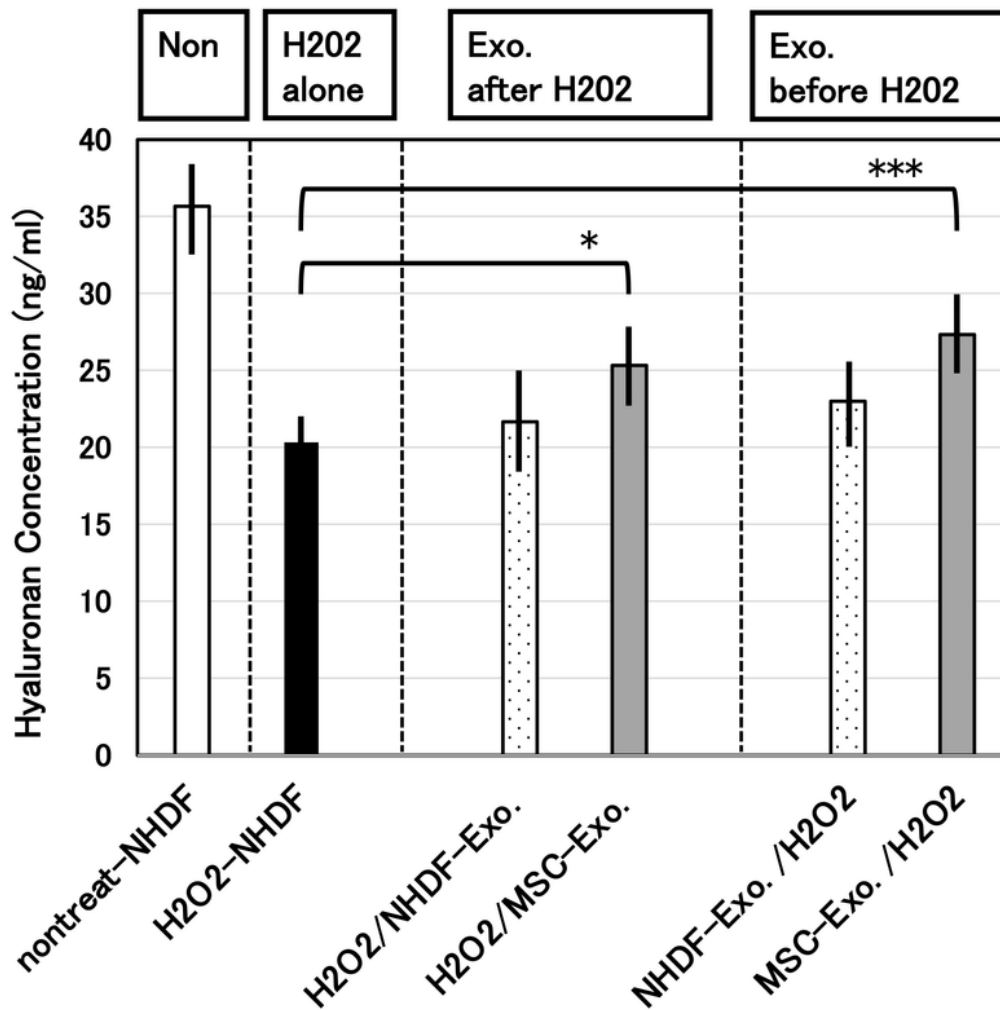


Figure 4

Hyaluronan secretion by normal human dermal fibroblasts (NHDFs). The amounts of hyaluronan released into the culture supernatant from NHDFs were measured via ELISA. *P < 0.05, *** P < 0.001.

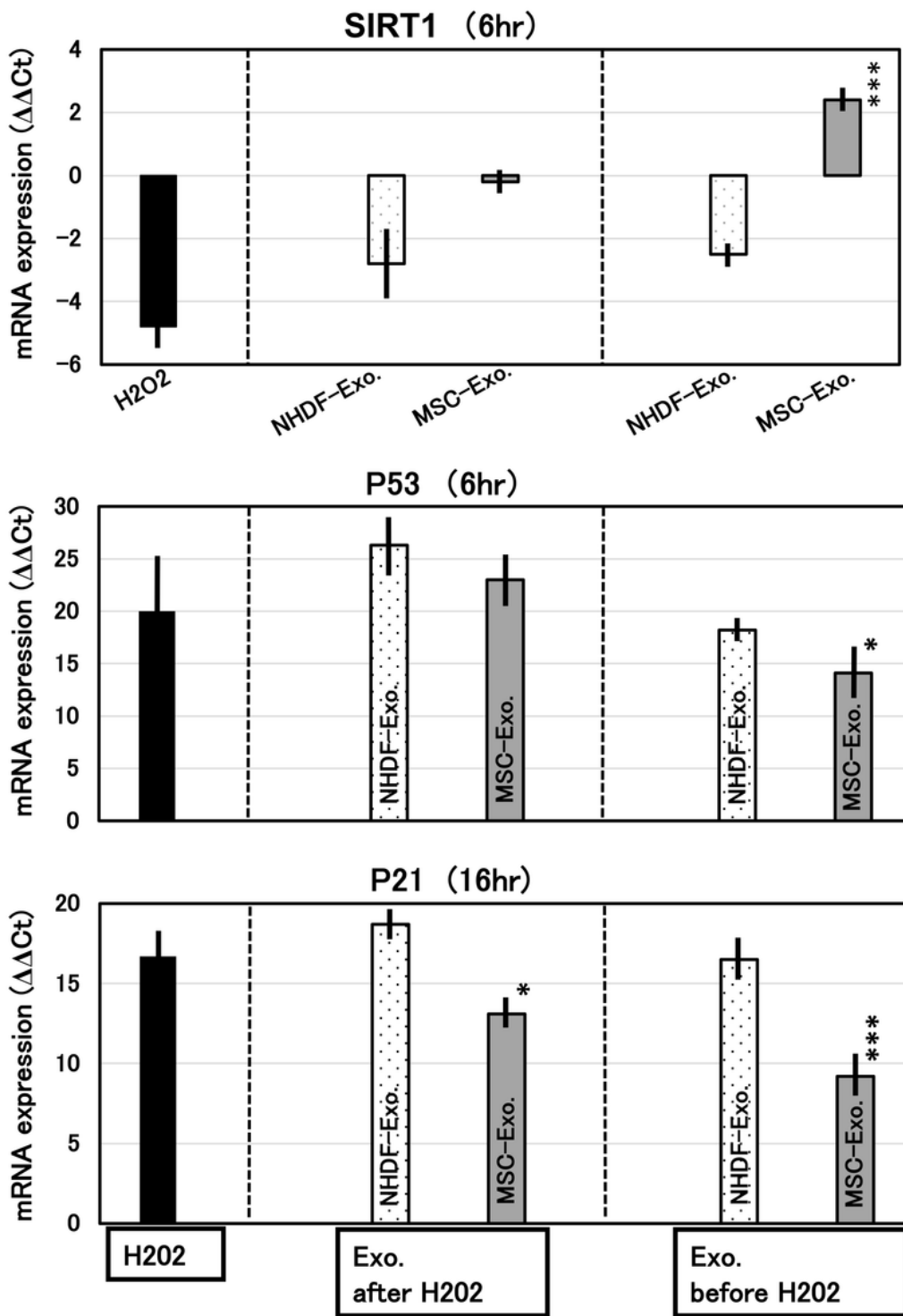


Figure 5

mRNA levels of cellular senescence-related genes in normal human dermal fibroblasts (NHDFs). The mRNA levels of SIRT1, p53, and p21 were determined by qRT-PCR and presented as $\Delta\Delta Ct$. * $P < 0.05$, *** $P < 0.001$.

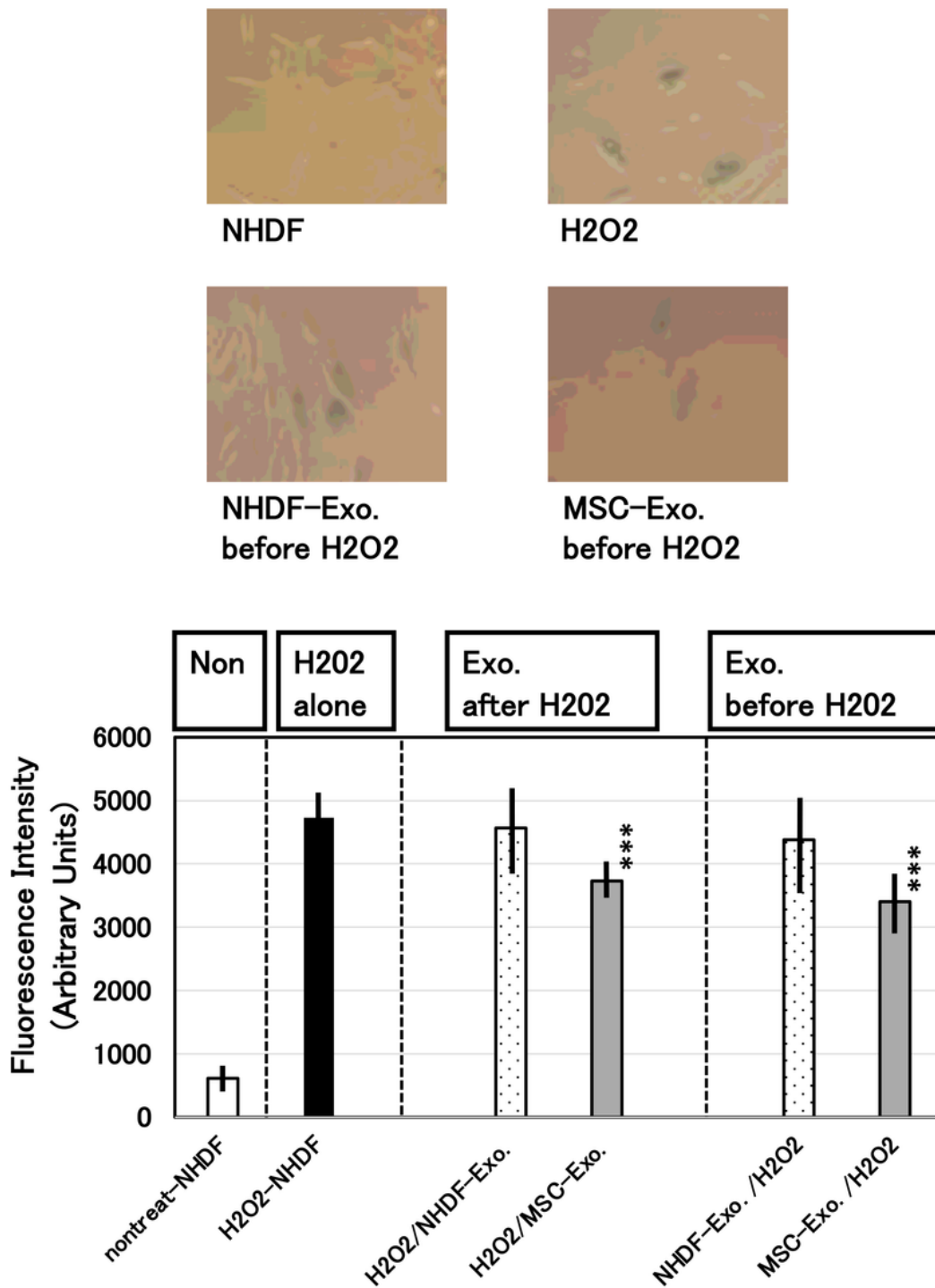


Figure 6

Inhibitory effects of mesenchymal stem cell exosomes (MSC-Ex) and normal human dermal fibroblast (NHDF) exosomes (NHDF-Ex) on cellular senescence. Cellular senescence was determined as β-galactosidase activity. Images of β-galactosidase activity are shown in the upper panels. The lower panel presents the quantitative data for intracellular β-galactosidase levels as determined via fluorescence intensity. ***P < 0.001 vs. H2O2-NHDF.

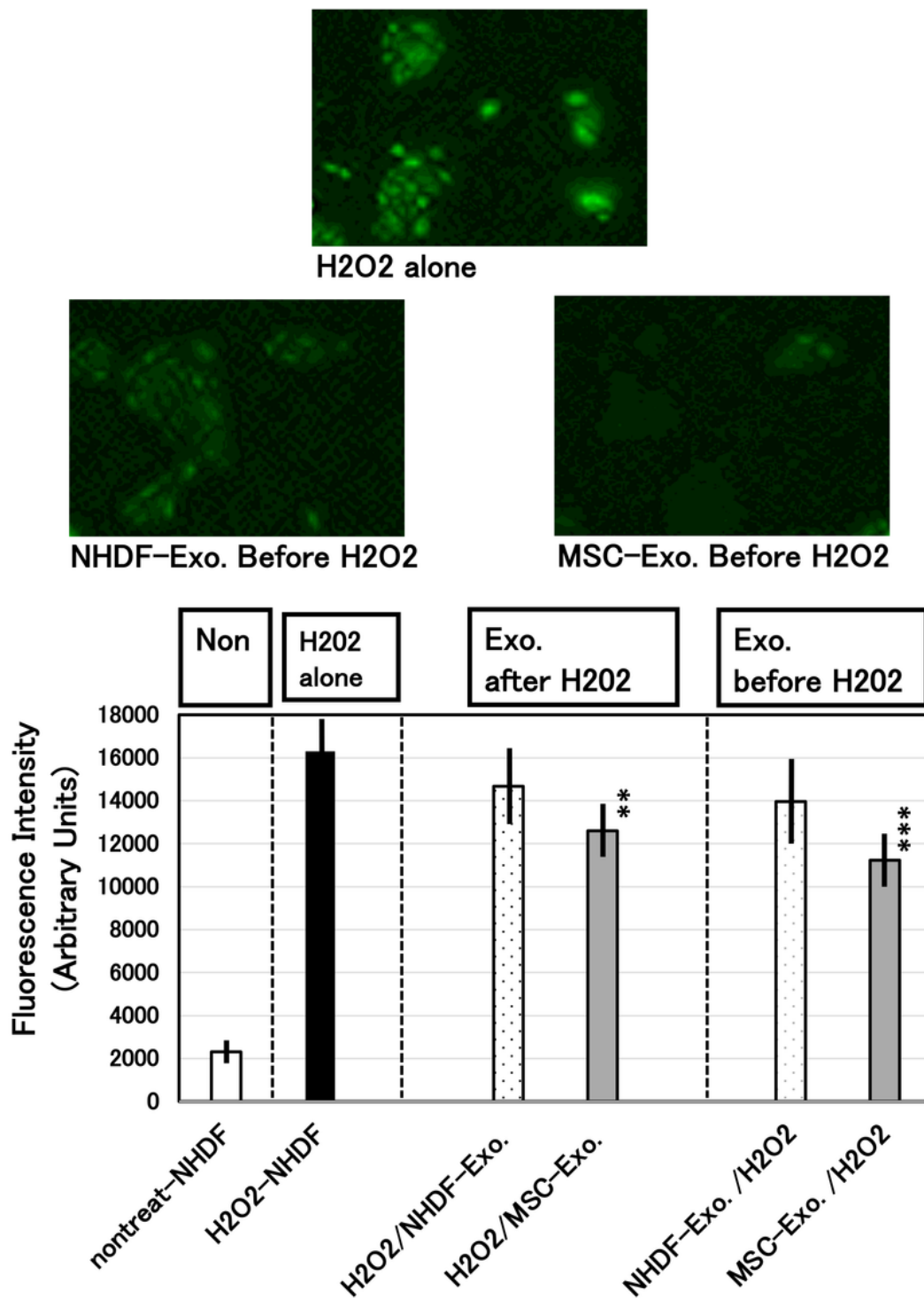


Figure 7

Inhibition of intracellular reactive oxygen species (ROS) generation by mesenchymal stem cell exosomes (MSC-Ex). After normal human dermal fibroblasts were treated with H2O2 and/or exosomes, ROS generation in the cell was detected using a fluorescent probe as described in the Materials and Methods, and images of ROS production are shown in the upper panels. The lower panel presents the quantitative

data for intracellular ROS production as determined via fluorescence intensity. **P < 0.01, ***P < 0.001 vs. H2O2-NHDF.